First publ. in: Applied Physics / A, Materials science and processing, 83 (2006), 1, pp. 1-3

I. KARAKURT[1,✉]
J. BONEBERG[2]
P. LEIDERER[2]

Electrochromic switching of WO_3 nanostructures and thin films

[1] Department of Physics, Isik University, Kumbaba Mevkii, 34980, Sile, Istanbul, Turkey
[2] Department of Physics, University of Konstanz, 78467, Konstanz, Germany

Received: 18 August 2005/Accepted: 12 November 2005
Published online: 4 January 2006 • © Springer-Verlag 2005

ABSTRACT We present transmission measurements through tungsten tri-oxide nanostructures and thin films prepared by sol–gel process on micro-contact printed substrates. Identical electrochromic switching times are found for both the nanostructures and the bulk films with equal thicknesses upon intercalation of H^+ ions. We attribute the large change in the transmission through nanostructures at 632 nm, which can not be solely explained by absorption, to diffraction effects.

PACS 73.40.Cg; 73.40.Mr; 78.20.-e; 78.67.n

1 Introduction

Electrical and optical properties of tungsten tri-oxide (WO_3) films can be modified reversibly. This material, which shows electrochromism, gasochromism, and photochromism, has applications in smart windows, rear view mirrors in automobiles and gas sensors. Electrochromism in WO_3, which involves ion/electron insertion and extraction, has been studied [1–3] widely since its discovery in 1973 by Deb [4]. Intercalation of metal ions (M^+) into tungsten oxide results in a tungsten bronze M_xWO_3. Usually, the intercalated ions are H^+, Li^+, K^+ and Na^+. Whereas a thin film of WO_3 is a transparent insulator, the tungsten bronze is a conductor and has a deep blue color. Amorphous films of W-oxide are infrared absorbing while sufficiently crystalline films are infrared reflecting [2]. The basic reason for the optical absorption is the formation of polarons [5, 6] around the W^{+5} sites in the oxide. The WO_3 is an interesting material which has been studied extensively in the form of thin films, but to our knowledge not as nanostructures. The question of how the physical properties change as one reduces the size of oxide structures has been left unexplored so far.

In this paper, we present a study of optical properties of tungsten oxide functional nanostructures. We find that the geometry does not play a role in the ion insertion mechanism, i.e., we do not see any difference in the switching time between bulk films of 25 nm thickness and the nanostructures with a height of 10 nm. Our measurements with both bulk films and dots show that the switching time is limited only by the potential barrier which must be overcome by the inserted ions at the electrolyte-oxide interface while the diffusion of the ions within the film seems to be much faster. Measurements of the transmission through the dots suggest that these periodic structures also act as a diffraction grating.

2 Sample preparation

In order to produce WO_3 samples, we prepared a sol solution by dissolving 1 g of WCl_6 in 10 ml ethanol. Upon mixing, a rapid reaction occurs and the solution takes an orange color which then changes slowly to clear-blue over fifteen to twenty minutes. We then waited about twelve hours for the chemical reactions, which result in the formation of tungsten alkoxide, to be completed. To prevent gelling by hydrolysis under ambient humidity, the sol was kept under Ar atmosphere in a closed vessel which allowed passing Ar over the sol to remove HCl vapor created during chemical reactions.

Thin films were prepared by spin-coating the tungsten alkoxide solution onto Au coated glass substrates. Producing the WO_3 nanostructures required patterning Au surfaces chemically prior to spin coating by the sol solution. Hydrophilic and hydrophobic regions were created on substrates through micro-contact printing using a combination of hydrophobic octadecanthiol ($HS(CH_2)_{17}CH_3$) and hydrophilic 11-mercaptoundecanol ($HS(CH_2)_{11}OH$). The transfer of the thiols onto the substrates was done using polydimethylsiloxane (PDMS) stamps which were cast from masters consisting of monolayers of 1 μm size colloidal polystyrene particles [7–9].

As for the production of the films, also for the nanostructures, right before the deposition, 0.5 ml/1 g–sol of Acetylaceton ($C_5H_8O_2$) was added to the sol solution as a surfactant to delay the gelation process. The samples were spun at 7000 rpm after allowing the sol to rest on the substrates for 20 s and then baked at 145 °C for one hour. We micro-contact printed only half of the surface of each substrate. Thus we were able to produce both oxide dots and bulk films on every substrate under the same preparation conditions. The data pre-

✉ Fax: +90-216-712-1474, E-mail: ikarakurt@isikun.edu.tr

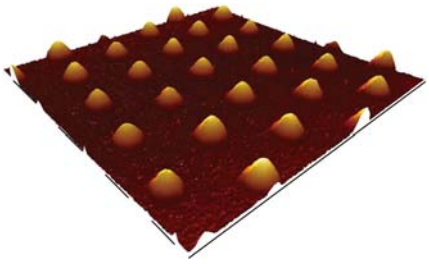

FIGURE 1 AFM image of tungsten tri-oxide dots formed on a chemically patterned (5×5 μm) Au surface. The *dots*, which are separated by 1 μm, have full width at half maximum (FWHM) of about 350 nm and a height of 8–10 nm

sented in this paper for bulk films and nanostructures were taken using different parts of the same sample. As an example of the nanostructures, we show an AFM picture of WO_3 dots formed on a chemically patterned surface of a Au substrate in Fig. 1. The dots form on the hydrophilic sites and have a height of 8–10 nm and a full width at half the maximum of about 350 nm. The thickness of the bulk film was also measured, after scratches were made on the film using a diamond tip, by AFM and found to be ~ 25 nm.

3 Experimental procedure

A schematic of the measurement setup is given in Fig. 2. As an electrolyte, 0.1 M HCl solution was chosen. A laser beam at 632 nm was focused onto selected parts of the sample by means of a converging lens. The diameter of the beam at the focus was about 10 μm. Focusing assures that only the part of the sample within the focus is probed by the photomultiplier. Samples were colored by biasing the Pt electrode positively with respect to the Au films which had a thickness of 75 nm. A reverse bias was used for the bleaching cycle.

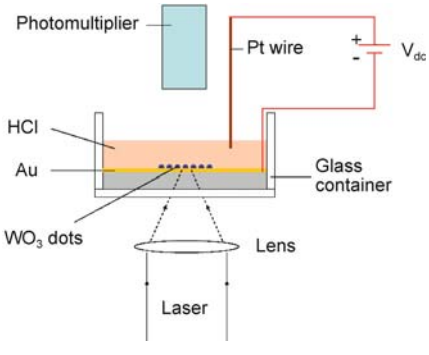

FIGURE 2 Setup for the measurements of the transmission through sol–gel prepared bulk film and dots. Distance between the sample and the detector is 4.8 cm. Lens-sample distance is 1.4 cm. Height of the electrolyte HCl is 1.6 cm

4 Results and discussion

In Fig. 3, we have plotted the transmission through both the bulk film and the dots as a function of time. The data shown are the average of nine cycles and normalized by the value of the transmission when the samples were bleached. For coloring, a voltage of $+1.75$ V was applied between $t = 0$ s and $t = 0.5$ s to the Pt electrode. A reverse bias of -1.75 V was applied between $t = 0.5$ s and $t = 3$ s for bleaching. Even though the absolute values of the transmission changes differ, the normalized data for the dots and the bulk film overlap extremely well as seen in the figure. The transmission for the dots (bulk) are plotted in gray (black) color. In the inset, both the coloring and the bleaching cycles are shown. The decay of the transmission upon switching is close to an exponential for both the bulk film and the dots. In order to describe the observed time dependence, we use the following equation

$$\frac{T}{T_0} = \frac{1}{T_0}\left[(T_0 - T_s)e^{-t/\tau} + T_s\right], \qquad (1)$$

where T_s is the transmission at saturation and T_0 is the transmission when the sample is in the bleached state. We obtain a switching time of $\tau = 38$ ms both for the bulk film and the dots. The change in the transmission between bleached and colored states is 7.6% for the bulk film. Estimating the expected change in transmission for the nanostructures yields a factor of 0.41 for the reduced thickness and a factor of 0.1 for the surface coverage. Thus the expected change would be 0.31% while the measurements give 1.55%. The unexpectedly large change in the transmission through the dots could be due to diffraction of the light into first order which is not collected by the photomultiplier. (Calculation shows that the diffraction into higher orders is not physically possible for the lattice spacing, the wavelength and the geometry of our setup.)

The different time dependencies of the transmission for coloring and bleaching cycles show that the charge injection dynamics are different during coloring and bleaching. This is consistent with earlier observations [10].

The switching time strongly depends on the bias voltage V_{dc} as shown in Fig. 4. The data presented in the figure are the results of the transmission measurements through bulk films. An applied voltage of 2.25 V results in a switching time of 12 ms. However as V_{dc} is increased, the stability of the sample after coloring and bleaching cycles worsens. At $V_{dc} = 2.25$ V, the number of coloring and bleaching cycles which can be achieved before the samples start

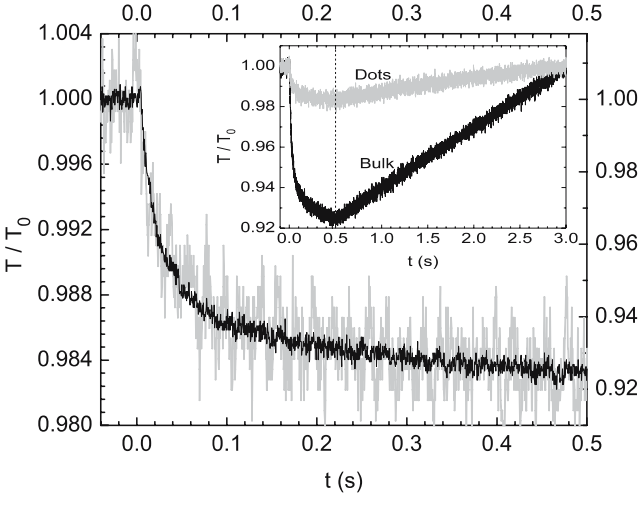

FIGURE 3 Normalized transmission, T/T_0, through sol–gel prepared WO_3 bulk film and the dots at 632 nm. The T_0 is the transmission when the sample is in the bleached state. The *left* and *the right ordinate axes* refer to the dots and the bulk film, respectively. Switching voltage $V_{dc} = 1.75$ V is turned on at $t = 0$. Identical switching times of $\tau = 38$ ms were measured for both the bulk film and the dots. The *inset* shows both the coloring and the bleaching cycles

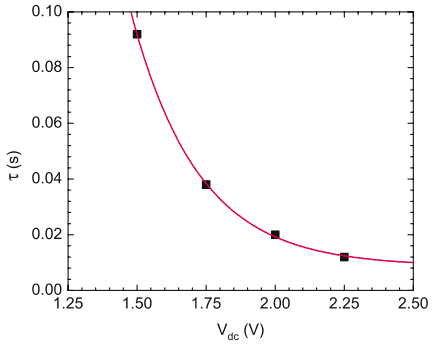

FIGURE 4 Switching time τ as a function of applied voltage V_{dc}. *Solid line* is an exponential fit as explained in the text

to dissolve is about 20. This number increases to 50 at $V_{dc} = 1.75$ V. We attribute the dissolution of the oxide to the stress which builds up as a result of insertion of H^+ ions. The rate of insertion increases exponentially with the applied voltage. In our measurement setup, we used a constant voltage source during coloring and bleaching cycles. In order for the oxide films and structures to be durable, the number of intercalated ions should be limited. However, with our setup, we were able to obtain a lower limit for the switching time as explained in the following. The data in Fig. 4 can be fitted to an exponential decay function given by

$$\tau(V) = \tau_1 e^{-V/V_0} + \tau_0 \,. \tag{2}$$

where V_0 corresponds to the potential barrier, which must be overcome by the H^+ ions entering into the oxide from the electrolyte at the electrolyte-oxide interface and τ_0 is the limit for the switching time when $V \gg V_0$. The agreement between the data and the fit to (2) is not surprising since exponential dependence is a well known signature of activated transport. The best fit in the figure was obtained for $\tau_1 = 40.4$ s, $V_0 = 0.242$ V, and $\tau_0 = 0.0086$ s. The potential barrier $V_0 = 0.242$ V agrees very well with the earlier measurements for H^+ ions [11]. We observe that the switching time is practically limited by V_0 and not by the diffusion of H^+ ions within the WO_3. The fit to the data shown in Fig. 4 gives, for the switching time τ, a lower limit of $\tau_0 = 0.0086$ s which is the average time it takes for the ion concentration gradient within the oxide to disappear after the start of coloring.

The diffusion constant D, as given by the Einstein relation, is

$$D = \frac{L^2}{\tau} \tag{3}$$

where τ is the average time it takes for the ions to diffuse a distance of L. Using $\tau = 0.0086$ s and $L = 25$ nm, we obtain a diffusion constant of $D \sim 7 \times 10^{-10}\,\mathrm{cm}^2/\mathrm{s}$ which is in agreement with earlier measurements for diffusion of H^+ ions in sol–gel prepared WO_3 films [11, 12]. The changes described so far are too small for application purposes. However, an increase of the dot thickness should increase the change in the transmission. In our experimental approach, the dot thickness is restricted by the liquid contact angle. Thus for the purpose of thicker structures new approaches have to be considered. An interesting idea stems from the polymer community and involves inducing phase separation in polymer mixtures by patterned surfaces [13]. Combining these ideas with sol–gel solutions should allow for the realization of thicker structures.

5 Conclusion

In summary, we have produced sol–gel prepared WO_3 nanostructures on chemically patterned substrates and showed that these structures are functional, i.e., they can be switched reversibly. We measured the transmission through sol–gel prepared periodic tungsten tri-oxide nanostructures in colored and transparent states and compared it with the measurements through bulk films. Switching times for both the dots and the bulk films are identical for the film thicknesses and the structures used in this study. The change in the transmission through the dots is greater than what is expected due only to absorption. We attribute this to diffraction effects. Although the switching times are the same for thin films and nanostructures, the outcome might be different for thicker structures when the diffusion time is larger than the time it takes for the intercalated ions to overcome the potential barrier at the electrolyte-oxide interface. Diffraction effects for oxide dots with larger heights should be studied.

ACKNOWLEDGEMENTS The authors would like to thank Clemens Bechinger for helpful discussions. This work was supported by the Kompetenznetz Funktionelle Nanostrukturen Baden-Württemberg and the Deutsche Forschungsgemeinschaft (SFB 513).

REFERENCES

1 C.G. Granqvist, *Handbook of Inorganic Electrochromic Materials* (Elsevier, Amsterdam 1995)
2 C.G. Granqvist, Solar Energy Mater. Solar Cells **60**, 201 (2000)
3 L. Berggren, A. Azens, G.A. Niklasson, J. Appl. Phys. **90**, 1860 (2001)
4 S.K. Deb, Phil. Mag. **27**, 801 (1973)
5 G.A. Niklasson, J. Klasson, E. Olson, Electrochem. Acta **46**, 1860 (2001)
6 D. Emin, PRB **48**, 13 691 (1993)
7 U.C. Fischer, H.P. Zingsheim, J. Vac. Sci. Technol. **19**, 881 (1981)
8 F. Burmeister, C. Schäfle, T. Matthes, M. Böhmisch, J. Boneberg, P. Leiderer, Langmuir **13**, 2983 (1997)
9 C. Bechinger, H. Muffler, C. Schäfle, O. Sundberg, P. Leiderer, Thin Solid Films **366**, 135 (2000)
10 C.G. Granqvist, Electrochem. Acta **44**, 3005 (1999)
11 M. Seman, C.A. Wolden, Solar Energy Mater. Solar Cells **82**, 517 (2004)
12 J. Wang, J.M. Bell, I.L. Skryabin, Solar Energy Mater. Solar Cells **56**, 465 (1999)
13 M. Böltau, S. Walheim, J. Mlynek, G. Krausch, U. Steiner, Nature **391**, 877 (1998)